# A legacy role for DNA binding of Lon protects against genotoxic stress

Rilee D. Zeinert[1#], Justyne L. Ogdahl[1], Jing Liu[1], Qiyuan Yang[2], Yunguang Du[2], Benjamin B. Barros[1], Peter L. Freddolino[3], Cole M. Haynes[2], Peter Chien[1*]

**Affiliations:**

[1]Department of Biochemistry and Molecular Biology, Molecular and Cellular Biology Program, University of Massachusetts Amherst, Amherst MA

[2]Department of Molecular, Cell and Cancer Biology. University of Massachusetts Medical School, Worcester MA

[3]Department of Biological Chemistry and Department of Computational Medicine & Bioinformatics, University of Michigan, Ann Arbor, MI 48109, USA

#current address: National Institute of Child Health and Human Development, 49 Convent Drive, Bethesda, MD 20892-4417

* pchien@umass.edu

**Abstract**

DNA binding proteins are essential for cellular life, but persistently bound complexes have toxic consequences. Here we show that the proteotoxic responsive bacterial protease Lon clears proteins from DNA to promote genotoxic stress resistance. Purified Lon binds DNA and degrades neighboring bound proteins, while a fully active DNA-blind Lon variant does not. This variant can degrade substrates as normal during unstressed growth, complements pleotropic phenotypes of Δ*lon*, including proteotoxic resilience, but remains sensitive to genotoxic stresses and fails to degrade proteins efficiently during DNA damage. Transposon sequencing reveals that Δ*lon* is vulnerable to loss of protein-DNA eviction factors and we use dynamic nucleoid occupancy profiling to show that chromosome-wide protein turnover relies on Lon DNA binding. Finally, disrupting Lon binding to mitochondria genomes also results in genotoxic stress sensitivity, consistent with the bacterial ancestry of this organelle. We propose that clearance of persistent proteins from DNA by Lon originated in free-living α-proteobacteria and maintained during the evolution of mitochondria.

**Summary**

DNA binding by the Lon protease protects against genotoxic damage in a manner preserved from bacteria to mitochondria.

## Introduction

Maintenance, replication, and readout of genomes requires DNA-binding proteins, which perform their functions with specific dynamics. However, proteins that dwell on DNA beyond their normal lifetimes can result in toxic consequences such as collisions of DNA polymerase with these roadblocks. Given that many proteins are known to be associated with the DNA, cells must have dedicated protein eviction pathways to prevent DNA-Protein roadblocks. In eukaryotes, chromatin remodeling factors evict nucleosomes and recent discoveries of the Sprtn proteases that remove covalently bound protein adducts from DNA represent the most extreme version of this process (Reinking et al., 2020). In bacteria, chromatin is condensed into the nucleoid which is highly occupied with both specific binding proteins (e.g., transcription factors) and less specific factors (e.g. HU, H-NS, etc). Like in eukaryotes, clearance of these proteins is needed, however, what factors collaborate to control this process in bacteria is less understood.

In bacteria, the AAA+ protease Lon degrades misfolded proteins (Goldberg, 1972; Gur and Sauer, 2008) and seminal work in *E. coli* revealed that loss of Lon sensitized cells to genotoxic stresses (Mizusawa and Gottesman, 1983; Witkin, 1946). Lon also plays a role during normal growth. For example, in the alpha-proteobacteria *Caulobacter crescentus (Caulobacter)*, the Lon protease degrades the epigenetic regulator CcrM (Wright et al., 1996), the transcriptional regulator SciP (Gora et al., 2013), and the replication initiator DnaA (Jonas et al., 2013), in addition to its role in protein quality control (Lu et al., 2007). However, whether Lon plays a role in genotoxic tolerance in bacteria other than *E. coli* remains poorly understood. In mitochondria, which have an alphaproteobacteria origin (Gray, 2012), Lon has been clearly shown to manage the response to protein misfolding but it is unclear if it regulates mtDNA stress responses (Bota and Davies, 2002; Lu et al., 2007; Nargund et al., 2012).

65 Intriguingly, early biochemical work with Lon shows that it can bind DNA (Charette et al., 1984;
66 Chung and Goldberg, 1982; Liu et al., 2004; Lu et al., 2007) and more recent work identified
67 specific residues important for DNA binding (Karlowicz et al., 2017), but the biological
68 consequences of this binding remains unclear.
69
70 Here we report that Lon binding to DNA is important for genotoxic stress responses but
71 not proteotoxic stress responses. Using transposon sequencing, we find that factors important
72 for evicting persistent protein complexes from DNA show synthetic fitness defects with loss of
73 Lon DNA binding. In vitro, purified Lon degrades neighboring proteins when bound to the
74 same DNA region and genome-wide proteome occupancy shows that Lon binding to DNA
75 affects the lifetime of proteins on the chromosome. Finally, we show the importance of Lon
76 DNA binding in genotoxic stress tolerance is preserved in mitochondria, highlighting the link
77 between these organelles and their $\alpha$-proteobacteria ancestor. Overall, our work supports a
78 model where Lon degrades lingering neighbor proteins when bound to chromosomal DNA, a
79 process that is especially important during the response to genotoxic stresses.
80
81 **Results**
82 *DNA binding of Lon is important for genotoxic stress tolerance*
83 We generated strains expressing only a DNA-blind variant of Lon (Lon4E) by mutating
84 residues implicated in DNA binding based on homology to the *E. coli* protein (Karlowicz et al.,
85 2017). Cells lacking Lon exhibit profound morphological defects including filamentation, loss of
86 motility in soft agar (Wright et al., 1996), and sensitivity to proteotoxic stresses such as
87 canavanine (Zeinert et al., 2020) (Figure 1A). Expression of Lon4E largely rescues these
88 phenotypes (Figure 1A,C; Figure S1). Unlike WT Lon, purified Lon4E fails to bind DNA (Figure
89 1B) but is completely active for degradation of model unstructured substrates such as casein
90 (Figure S1). *In vivo*, loss of Lon results in increased levels of its substrates DnaA and CcrM

91 (Jonas et al., 2013; Wright et al., 1996) and Lon4E restores steady-state levels to essentially
92 wildtype levels (Figure S1).

93
94 Interestingly, although they are resistant to proteotoxic stresses, Lon4E strains remain
95 sensitive to DNA damaging stresses, most particularly genotoxic agents that yield complex
96 damages such as mitomycin C (Figure 1A). Consistent with this, the prolific filamentation upon
97 DNA damage associated with ∆lon strains is also seen with Lon4E but not WT strains (Figure
98 1C). Our general interpretation is that the Lon4E allele is fully capable of complementing
99 wildtype Lon activity during normal and proteotoxic stress but fails to fully protect against
100 genotoxic stress.
101
102 *Loss of protein eviction factors is synthetically sick with loss of Lon activity*
103 We had previously used transposon sequencing to identify genes that are differentially
104 critical in a Lon-dependent manner (Figure 2A; (Zeinert et al., 2020)). Given the extreme
105 sensitivity of Lon-deficient strains to genotoxic agents (Figure 1), we hypothesized that many
106 members of the DNA damage response (DDR) pathway would be essential in ∆*lon*. However,
107 we found that most genes in the DDR were unaffected, including the sentinel protein RecA,
108 translesion polymerase (*imuB*) and mitomycin C specific responders (*mmcA*) (Figure 2 A,B),
109 which we confirmed by generating viable double mutants (Figure 2 C).
110
111 Only two DDR genes passed our filter as more essential in a ∆*lon* background (Figure 2
112 A,B). The first of these is *uvrD*, a helicase originally known for its role in DNA damage repair
113 (Ogawa et al., 1968). UvrD can evict proteins bound to DNA, such as disassembling RecA
114 nucleofilaments (Petrova et al., 2015; Veaute et al., 2005) and stalled RNAP complexes
115 (Epshtein et al., 2014). While we could delete *uvrD* from wildtype cells, we could not delete *uvrD*

116 from Δ*lon* cells and depletion of Lon in a Δ*uvrD* strain was lethal (Figure 2C). Similarly, we found
117 *xseB*, a subunit of exonuclease VII that is important for reactivation of stalled replication forks
118 and mismatch repair (Lovett, 2011) also results in synthetic sickness when Lon is depleted
119 (Figure 2C; Figure S2).
120
121 One pathway where UvrD and ExoVII converge is in clearing protein roadblocks from DNA
122 (by UvrD) before they cause stalling of replication forks that must be restarted (initiated by
123 XseB). Interestingly, while Lon4E strains were equally fit as wildtype strains under normal
124 conditions, loss of UvrD in a Lon4E background compromised growth compared to the parental
125 Δ*uvrD* strain (Figure 2D). Taken together, we hypothesize that Lon binding to DNA aids in the
126 clearance of bound proteins, a function of particular importance during response to DNA
127 damage. We therefore looked at how protein dynamics *in vivo* could be affected by Lon DNA
128 binding.

129

130 *Lon binding to DNA affects condition dependent protein degradation*
131 Degradation of known Lon substrates, such as DnaA and CcrM, during nondamaging
132 conditions was the same in Lon4E strains as wildtype (Figure 3A). However, when MMC was
133 added to induce DNA damage, wildtype cells maintained robust DnaA turnover, while in
134 Lon4E, DnaA is degraded at ~50% of the wildtype rate. This stabilization did not extend to a
135 different Lon substrate, CcrM (Figure 3A), nor was this effect seen with the ClpXP substrate
136 CtrA (Jenal and Fuchs, 1998; Joshi et al., 2015) (Figure S3).
137
138 *In vitro*, purified Lon degrades DnaA poorly on its own consistent with prior work showing
139 that unfolded substrates activate Lon degradation of DnaA (Jonas et al., 2013). Interestingly,
140 addition of a dsDNA with canonical DnaA binding sites results in robust degradation of DnaA

141 by Lon (Figure 3C). This effect required both an intact DnaA binding motif and a sufficiently
142 long adjacent region for Lon to bind as well (Figure 3C). Consistent with a requirement for
143 DNA binding by Lon for this activity, purified Lon4E does not degrade DnaA as well as
144 wildtype in the presence of this dsDNA scaffold (Figure S3). We conclude that Lon binding to
145 DNA is needed for robust degradation of neighboring substrates, such as DnaA, an effect
146 particularly important during genotoxic stress.
147
148 *Locus specific protein occupancy of the chromosome is regulated by DNA binding of Lon*
149 Our working model is that DNA binding AAA+ proteases like Lon can clear persistent
150 protein complexes. If this is true, then Lon mutants deficient in DNA binding should show
151 persistent protein occupancy on the chromosome. To explore this, we used a modification of
152 IPOD, a technique where fragmented crosslinked protein-DNA is purified and sequenced to
153 reveal protein occupancy of the bacteria chromosome (Freddolino et al., 2021). We monitored
154 chromosome occupancy in wildtype and Lon4E strains following translation inhibition, to reveal
155 loci where DNA-bound proteins are removed by AAA+ proteases.
156
157 Our dynamic IPOD approach revealed many regions of the chromosome that become
158 less occupied after translational inhibition in a wildtype strain - many of these regions
159 remained occupied in a Lon4E strain after similar treatment (Figure 3D). Correlation analyses
160 show that the occupancies of pre-inhibition wildtype, pre-inhibition Lon4E, and post-inhibition
161 Lon4E were more like each other compared to the occupancy seen in the wildtype post-
162 inhibition sample (Figure 3C). Closer examination of occupancy data suggests a role for Lon
163 clearing gene regulatory regions, such as those present in the promoter regions of *ccrM* and
164 CCNA_02622, a putative amidase located adjacent to *ftsZ* (Figure 3D). Taken together, these
165 data suggest that regions of the genome are bound with proteins that are cleared by Lon when
166 it binds to DNA.

167

168 *DNA binding properties of Lon are important for genotoxic stress responses in mitochondria*

169 Mitochondria have an endosymbiotic origin (Margulis, 1970) and the current model is
170 that a free-living alpha-proteobacterium was engulfed by the ancestor of the modern
171 eukaryotic cell (Gray, 2012). Because *Caulobacter* is an $\alpha$-proteobacteria, we explored if the
172 need for DNA binding of Lon in tolerating DNA damage was preserved in mitochondria. In *C.*
173 *elegans*, mitochondrial Lon (LONP-1) is required for development and growth (Nargund et al.,
174 2012). Based on homology, we engineered a variant of *lonp-1* with mutations in the
175 corresponding predicted DNA binding residues to generate LONP-1$^{4E}$ and used CRISPR/Cas9
176 to produce worms expressing only this allele at the endogenous locus. Importantly, we found
177 that worms expressing only the LONP-1$^{4E}$ variant at endogenous levels were healthy, grew
178 and developed normally (Figure 4A,D). Because LONP-1 has a known role in mitochondrial
179 protein quality control by recognizing and degrading diverse proteins that incur oxidative
180 damage (Bota and Davies, 2002), we infer that LONP-1$^{4E}$ is capable of maintaining
181 proteostasis during animal development. Pull-down experiments indicated that LONP-1
182 robustly binds mitochondrial genomes *in vivo* as previously suggested (Fu et al., 1997; Lu et
183 al., 2007), but LONP-1$^{4E}$ does not (Figure 4B). Therefore, DNA binding of mitochondria Lon is
184 not essential for normal development or growth.

185

186 The mitochondrial unfolded protein response (UPR$^{mt}$) couples the state of mitochondrial
187 protein homeostasis to an upregulation of nuclear encoded chaperone genes. Induction of the
188 UPR$^{mt}$ requires the transcription factor ATFS-1, which is targeted to the nucleus when
189 mitochondria undergo stress. Complete depletion of LONP-1 activates the UPR$^{mt}$, as
190 determined by upregulation of the transcriptional mitochondrial chaperone reporter *hsp-6$_{pr}$::gfp*
191 (Yoneda et al., 2004) (Figure 4C) consistent with a role for LONP-1 in the maintenance of
192 mitochondrial function (Nargund et al., 2012). LONP-1$^{4E}$ worms do not activate the UPR$^{mt}$

193 suggesting mitochondrial protein homeostasis is intact (Figure 4D). However, LONP-1$^{4E}$
194 worms exposed to cisplatin showed a dramatic activation of UPR$^{mt}$ that is ATFS-1 dependent
195 while wildtype worms show no response (Figure 4D). Importantly, mitochondrial dysfunction
196 driven by depletion of the protein quality control protease SPG-7 caused UPR$^{mt}$ activation in
197 both wildtype and LONP-1$^{4E}$ animals to the same degree (Figure 4E), as does exposure to
198 paraquat which induces mitochondrial oxidative stress (Figure 4E). These results show that,
199 similar to what is seen in *Caulobacter*, loss of DNA binding of Lon in mitochondria results in a
200 specific intolerance to genotoxic stress.
201
202 **Discussion**
203 The role of DNA binding in Lon has been enigmatic since its initial observation (Chung
204 and Goldberg, 1982; Zehnbauer et al., 1981). Our working model is that Lon binding to DNA
205 allows it to recognize neighboring proteins and serves as an additional layer of quality control
206 to reduce the residence time of persistent DNA binding complexes (Figure 4F). This oversight
207 works in concert with other protein eviction factors such as UvrD and seems particularly
208 important during DNA damaging conditions (Figure 4F). Using a genome wide approach, we
209 find evidence for clearance of protein complexes during normal growth that relies on Lon
210 binding to DNA. Finally, we have shown that the same properties of DNA binding in Lon that
211 are important for genotoxic stress responses in *Caulobacter* are also important in
212 mitochondria, consistent with the endosymbiotic $\alpha$-proteobacteria ancestry of this organelle.
213
214 Overall, our working model is that Lon plays a canonical role in proteotoxic stress
215 response by degrading misfolded or damaged proteins. This function occurs regardless of
216 DNA binding. However, DNA binding of Lon also allows for local control of neighboring
217 proteins that is particularly important during genotoxic stress conditions. Our working model is
218 that Lon clearance of persistently bound proteins prevents the accumulation of protein

219 roadblocks that limit replication or transcription. This is particularly important in bacteria and
220 bacterially derived organelles, as replication, transcription and translation occur concurrently in
221 the same compartment. Because Lon recognizes substrates based on general chemical
222 properties as opposed to highly specific sequence motifs, Lon would be ideally suited to serve
223 in this capacity as the identity of the protein roadblock will likely depend on the specific
224 circumstance that generated it.

225

226 **Figure Legends**

227 **Figure 1**. **A**. Serial dilutions (10-fold dilutions left to right) of wildtype (WT), Lon deficient
228 (Δ*lon*), or DNA binding deficient Lon expressing (Lon4E) strains on media containing various
229 concentrations of either proteotoxic (L-canavanine (L-can)) or genotoxic (mitomycin C (MMC),
230 cisplatin (Cis), methyl methanosulfone (MMS), 4-nitroquinolone (4NQO)) compounds. **B.** Lon
231 binding to fluorescently labeled DNA oligo as measured by change in fluorescence
232 polarization. Data was fit to a hyperbolic binding model, $K_D$= 286 nM (95% CI: 90-1200 nM).
233 Concentration is reported as hexamers of Lon. inset: polarization measurement of labeled
234 DNA in the presence of wildtype Lon or Lon4E. **C.** Morphology of cells during normal growth
235 and after damaging with mitomycin C. Scalebar showing 5 μm in first panel, all other panels
236 are the same magnification.

237

# Figure 1

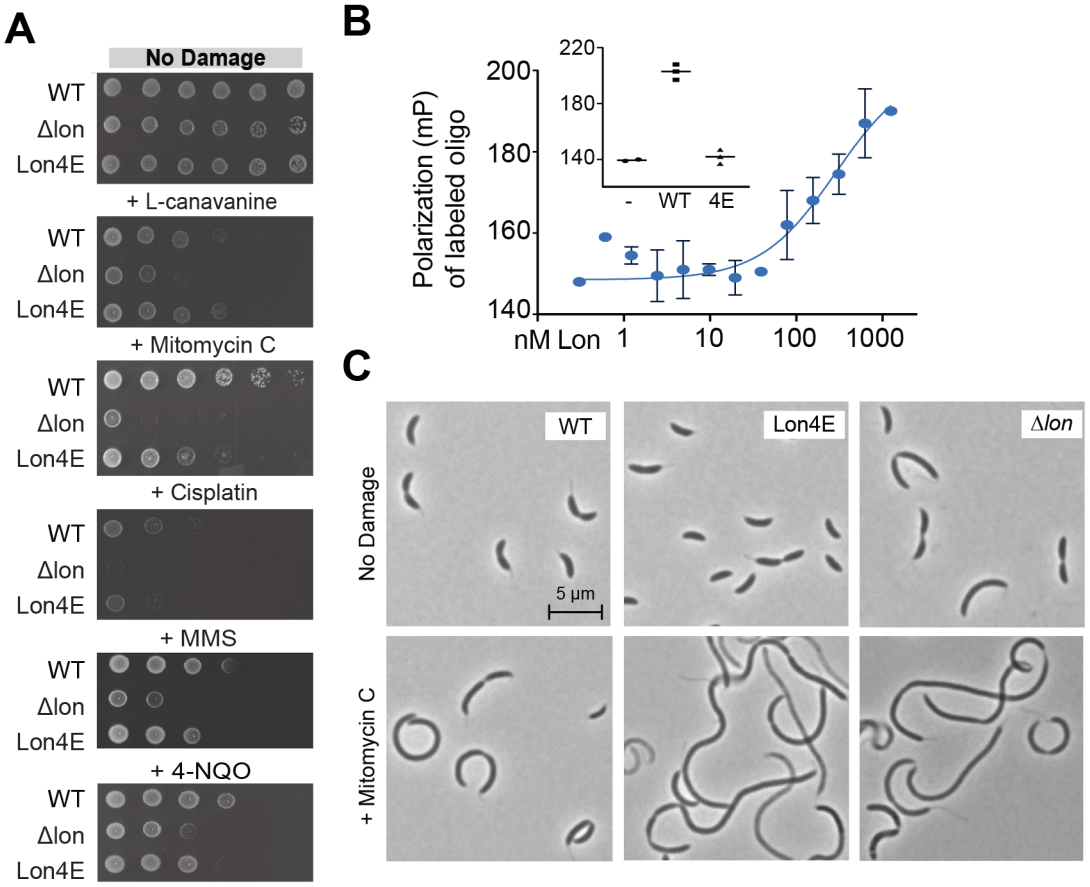
A
No Damage
WT
Δlon
Lon4E
+ L-canavanine
+ Mitomycin C
+ Cisplatin
+ MMS
+ 4-NQO
B
Polarization (mP) of labeled oligo
200
180
160
140
nM Lon
1
10
100
1000
220
180
140
-
WT
4E
C
No Damage
+ Mitomycin C
WT
Lon4E
Δlon
5 µm

238 **Figure 2. A.** Transposon-sequencing reveals genes that differentially affect fitness in wildtype
239 or ∆lon strains (Zeinert et al., 2020), highlighting genes annotated as DNA damage repair
240 genes (red). **B.** Snapshots of transposon insertion sites for DNA damage repair genes in
241 either wildtype (WT) or ∆lon strains. **C.** above: Induction (+) or depletion (-) of Lon in either
242 wildtype, ∆uvrD, or ∆exoVII strains, showing synthetic sickness. below: Deletions of DNA
243 damage repair genes *recA*, *imuB*, or *mmcA* can be generated in ∆lon strains without loss of
244 viability and as expected are generally important for response to MMC. D. Lon4E strains
245 grow as well as wildtype based on competition, but deletion of *uvrD* reduces fitness in a Lon4E
246 background.
247

**Figure 2**

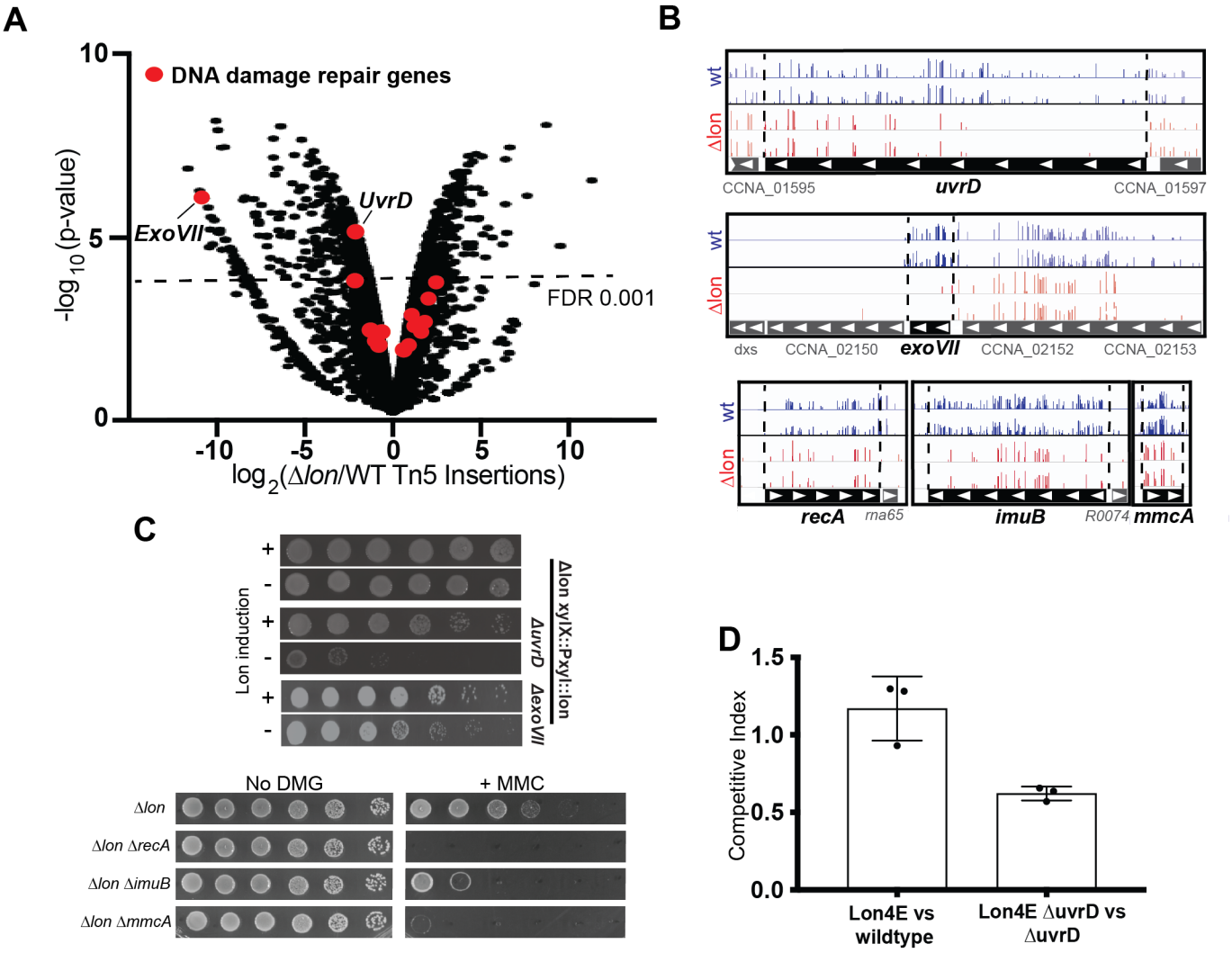
A
DNA damage repair genes
ExoVII
UvrD
FDR 0.001
-log10(p-value)
log2(Δlon/WT Tn5 Insertions)
B
wt
Δlon
CCNA_01595
uvrD
CCNA_01597
dxs
CCNA_02150
exoVII
CCNA_02152
CCNA_02153
recA
rna65
imuB
R0074
mmcA
C
Lon induction
Δlon xylX::PxylI::lon
ΔuvrD
ΔexoVII
No DMG
+ MMC
Δlon
Δlon ΔrecA
Δlon ΔimuB
Δlon ΔmmcA
D
Competitive Index
Lon4E vs wildtype
Lon4E ΔuvrD vs ΔuvrD

248

249 **Figure 3. A.** Degradation of DnaA and CcrM in wildtype, Lon4E or ∆lon strains as monitored
250 by translational shutoff experiments either in nondamaging or DNA damaging (+Mitomycin C)
251 conditions. B. Cartoon illustrating dsDNA oligonucleotides used to test for scaffolding. C.
252 Degradation of purified DnaA by Lon in the presence of different dsDNA scaffolds. D.
253 Spearman correlation matrix of genome occupancy in wildtype (WT) or strains expressing
254 Lon4E (Lone4E) as monitored by IPOD (Freddolino et al., 2021) either before (Pre) or two
255 hours after (Post) translational shutoff. Degree of correlation is shown by color and inset
256 values. E. Representative tracks showing changes in protein occupancy at *ftsZ* and *ccrM*
257 neighboring regions in either WT or Lon4E strains.

258

# Figure 3

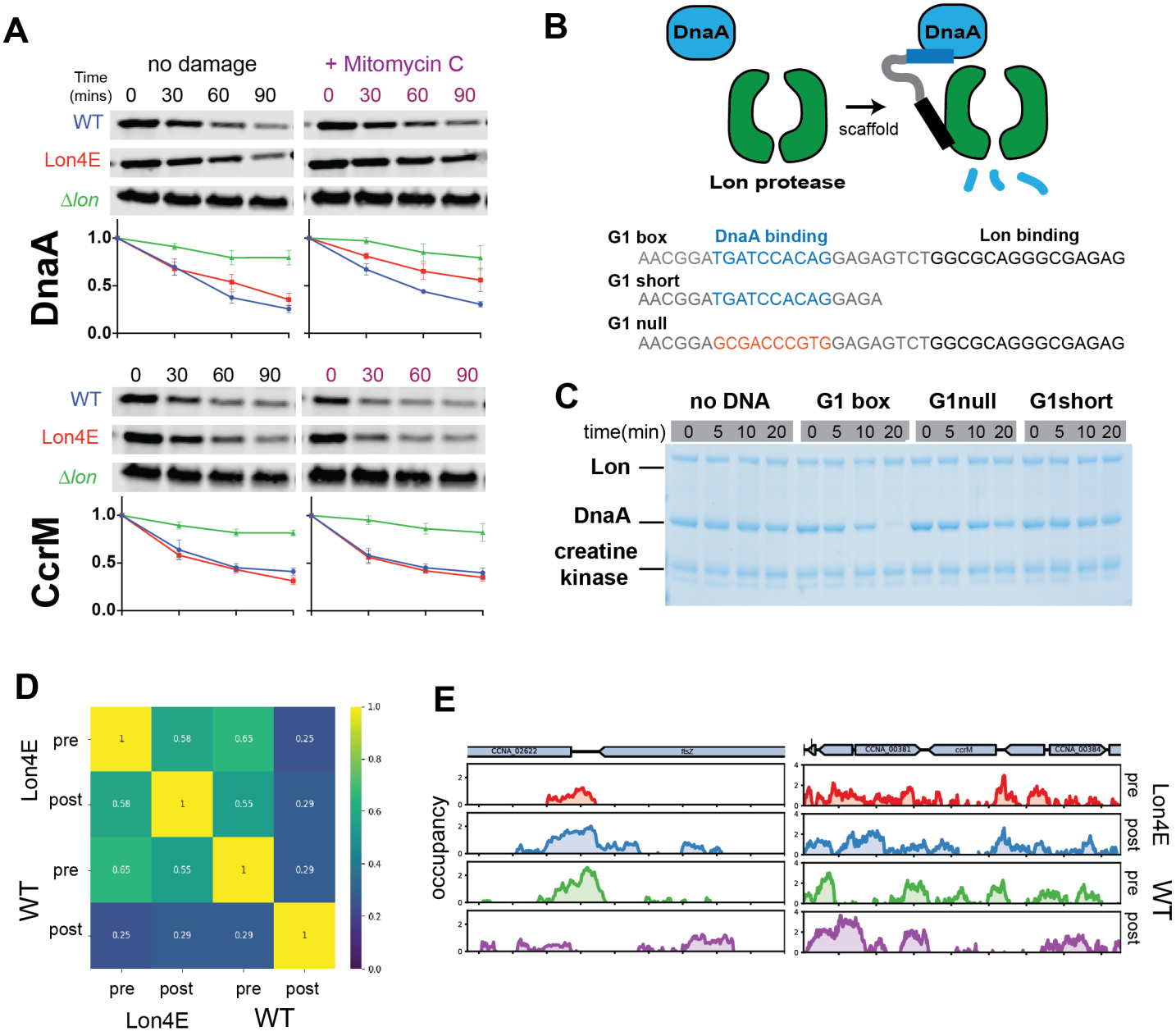
A
no damage
+ Mitomycin C
Time (mins)
0 30 60 90
0 30 60 90
WT
Lon4E
Δlon
DnaA
1.0
0.5
0.0
CcrM
B
DnaA
DnaA
scaffold
Lon protease
G1 box
DnaA binding
Lon binding
AACGGATGATCCACAGGAGAGTCTGGCGCAGGGCGAGAG
G1 short
AACGGATGATCCACAGGAGA
G1 null
AACGGAGCGACCCGTGGAGAGTCTGGCGCAGGGCGAGAG
C
no DNA
G1 box
G1null
G1short
time(min)
0 5 10 20
Lon
DnaA
creatine kinase
D
Lon4E
WT
pre
post
1
0.58
0.65
0.25
0.58
1
0.55
0.29
0.65
0.55
1
0.29
0.25
0.29
0.29
1
1.0
0.8
0.6
0.4
0.2
0.0
Lon4E
WT
E
CCNA_02622
ftsZ
CCNA_00381
ccrM
CCNA_00384
occupancy
pre
post
Lon4E
WT

259

260 **Figure 4.** DNA binding mutants of mitochondria Lon. **A**. Immunoblots of lysates from WT
261 worms, or strains expressing LONP-1-FLAG or LONP-$1^{4E}$-FLAG. Tubulin serves as a loading
262 control. **B**. ChIP of mtDNA with FLAG antibody in WT, LONP-1-FLAG and LONP-$1^{4E}$-FLAG
263 strains. **C.** Cartoon illustrating hsp-6 reporter of mitochondria stress. **D.** Photomicrographs of
264 *hsp-6$_{pr}$::gfp* WT or LONP-$1^{4E}$ worms raised on DMSO or cisplatin, scale bar, 0.5 mm. **E.**
265 Photomicrographs of *hsp-6$_{pr}$::gfp* WT or LONP-$1^{4E}$ worms raised on paraquat (PQ) or *spg-*
266 *7*(RNAi). **F.** Model for how Lon binding to DNA clears persistent proteins (gray) together with
267 other evicting enzymes such as UvrD (red).

268

# Figure 4

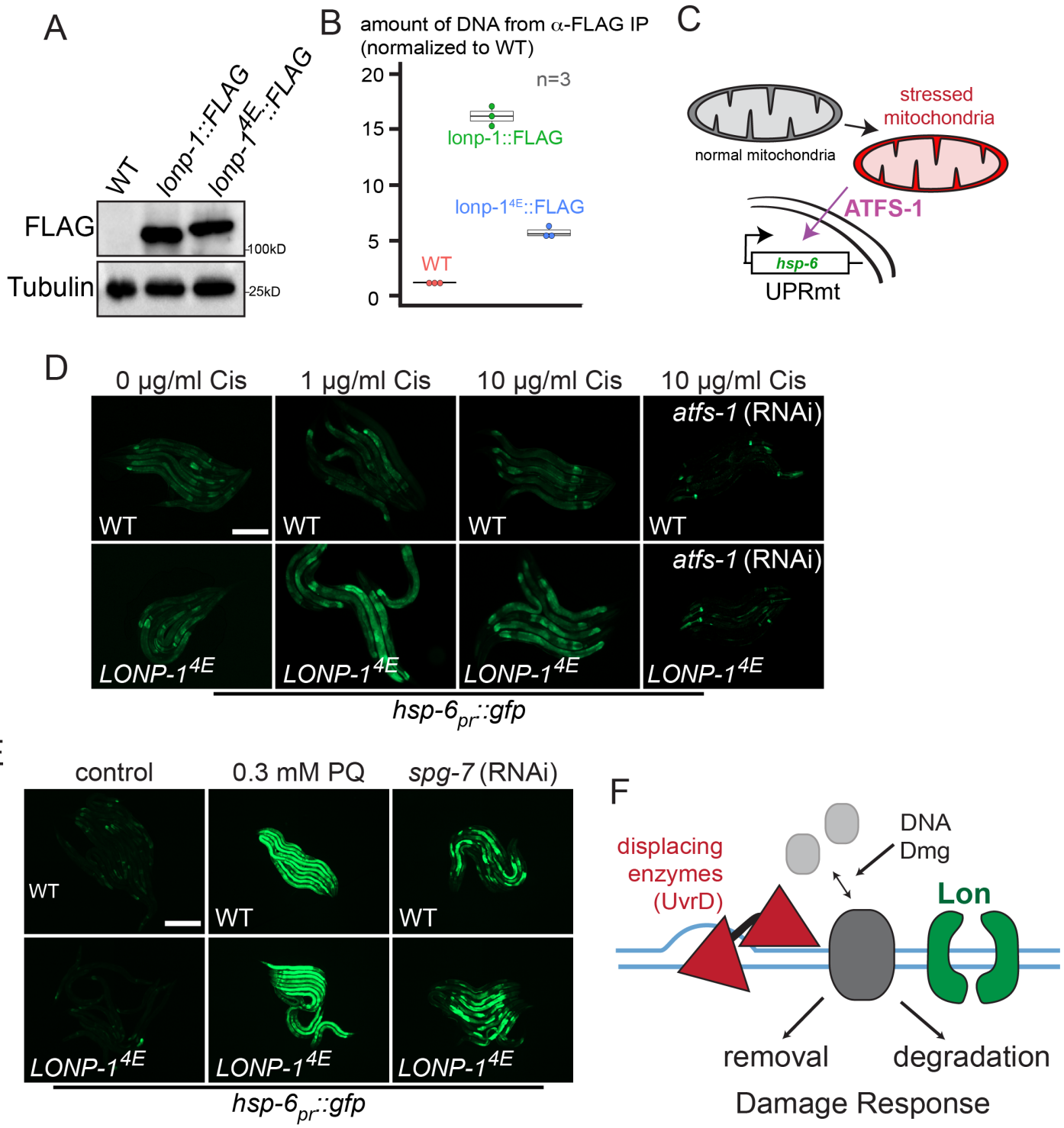
A
WT
lonp-1::FLAG
lonp-1^4E::FLAG
FLAG
Tubulin
100kD
25kD
B
amount of DNA from α-FLAG IP
(normalized to WT)
n=3
lonp-1::FLAG
lonp-1^4E::FLAG
WT
20
15
10
5
0
C
normal mitochondria
stressed mitochondria
ATFS-1
hsp-6
UPRmt
D
0 µg/ml Cis
1 µg/ml Cis
10 µg/ml Cis
10 µg/ml Cis
atfs-1 (RNAi)
WT
LONP-1^4E
hsp-6pr::gfp
E
control
0.3 mM PQ
spg-7 (RNAi)
WT
LONP-1^4E
hsp-6pr::gfp
F
displacing enzymes (UvrD)
DNA Dmg
Lon
removal
degradation
Damage Response

**Acknowledgements:**

We thank Lucy Shapiro for supplying the anti-CcrM antibody and members of the Chien lab and the Protein Homeostasis theme of the Center for Models to Medicine for helpful feedback. **Funding:** This work was supported by HHMI (C.M.H.), the Mallinckrodt Foundation (C.M.H) and National Institutes of Health grants (R01AG040061) to C.M.H. and (R35GM130320) to P.C. R.Z. and J.L. were funded in part by the UMass Chemistry Biology Interface Training Program (NIH T32GM139789). J.O. was funded in part by the UMass Biotechnology training program (NIH T32GM135096). **Author contributions:** P.C., J.L., and R.Z. conceptualized the study. B.B., J.L., J.O., R.Z, Q.Y., and Y.D. performed experiments. P.C., C.H., R.Z, and J.L wrote the initial draft. All authors reviewed the final draft. **Data and materials availability**: All data is available in the main text or the supplementary materials.

282

283 **Materials and Methods**

284 Bacteria strains and media

285 *C. crescentus* was grown on peptone yeast extract (PYE) at 30°C. 1.5% agar was used for
286 solid media. Carbon sources were supplemented at final concentrations of 0.2% glucose or
287 xylose. Antibiotics were used at the following concentrations for solid media growth:
288 Kanamycin 25 μg/ml, Spectinomycin 100 μg/ml, Tetracycline 1.5 μg/ml and Gentamycin 25
289 μg/ml. For growth of *E. coli* in solid or liquid media, we used lysogeny broth (LB) at 37°C.
290 Antibiotics were used at the following concentrations: Chloramphenicol 30 μg/ml, Kanamycin
291 50 μg/ml, Tetracycline 15 μg/ml and Gentamycin 50 μg/ml. After initial selection steps for
292 strain construction, antibiotic selection was excluded from all physiological related studies.

293

294 Strain construction

295 Deletion strains were constructed using the two-step recombination procedure with counter
296 selection by sucrose/*sacB*, using pNPTS138 plasmids containing deletion cassettes
297 comprised of 1000 bp upstream and downstream of the coding regions flanking a gentamycin
298 resistance cassette. Following transformation, initial primary selection was on PYE with
299 Kanamycin 25 μg/ml. Primary colonies were grown overnight in PYE without selection to allow
300 for secondary recombination. Overnight cultures were plated onto solid media supplemented
301 with 3% (w/v) sucrose and 25 μg/ml Gentamycin. To validate gene deletion, resulting strains
302 were tested for antibiotic sensitivity to Kanamycin and resistance to Gentamycin. Phage
303 transduction of marked alleles was performed using PhiCr30.

304

305 Allelic replacement of Lon4E was performed by transforming pNPTS138-Lon4E into CPC546
306 (lon::specR) with primary selection on PYE with Kanamycin 25 μg/ml and secondary selection

307 on PYE + 3% (w/v) sucrose. The resulting strains were genotyped for antibiotic sensitivity to
308 Kanamycin and Spectinomycin. Clones harboring the correct genotype were then confirmed
309 by PCR amplification of the *lon* locus, Sanger sequencing, and whole genome resequencing of
310 the strain.
311
312 Protein Purification and *in vitro* degradation assays
313 Lon, Lon4E, and DnaA were purified with protocols as previously described (Jonas et al.,
314 2013) using hydroxyapatite resin (Sigma) instead of P11 cellulose for Lon/Lon4E.

315 FITC casein degradation was performed as previously described (Vieux et al., 2013). Briefly,
316 degradation assays (30°C) were as follows unless noted otherwise: Lon/Lon4E hexamer 0.15
317 μM, 10 μg/ml FITC casein type II (Sigma), ATP 4 mM, 75 μg/ml creatine kinase, 5mM creatine
318 phosphate. Final concentrations of components in degradation assays (30°C) were as follows
319 unless noted otherwise: Lon/Lon4E 0.15 μM (hexamer concentration), DnaA 2.5 μM, DNA 2
320 μM, ATP 4 mM, 75 μg/ml creatine kinase, 5 mM creatine phosphate.

321 Fluorescent polarization studies
322 ssDNA (AACGGATGATCCACAGGAGAGTCTGGCGCAGGGCGAGAG) labeled with
323 fluorescein (FAM) was ordered from Integrated DNA Technologies. Wildtype Lon was titrated
324 in two-fold dilutions starting from 1.25 μM (all concentrations in hexamer). For inset in Figure
325 1, 300 nM of Lon or Lon4E hexamer was incubated with 200nM FAM-DNA in 20mM HEPES,
326 10mM $MgCl_2$, 100mM KCl with 0.05% Tween. Polarization measurements were read from 40
327 uL of these mixtures using opaque non-binding black 384-well plates (Corning) and a
328 SpectraMax M5 plate reader (Molecular Devices), with excitation and emission wavelengths
329 set at 460 nm and 540 nm respectively.
330

331

332 Bacteria Characterization: Motility, Morphology, Viability and Stress Assays

333 For motility assays, single colonies were picked from PYE agar and inoculated into 0.3% PYE

334 agar. Plates were grown at 30°C for 2 days before imaging.

335

336 Microscopy images are phase contrast images of exponentially growing *Caulobacter* cells

337 $OD_{600} \approx 0.4$ (Zeiss AXIO ScopeA1) mounted on 1% PYE agar pads using a 100X objective.

338

339 Caulobacter strains were cultured in PYE medium overnight. Cultures were diluted to $OD_{600}$

340 0.05 and grown to $OD_{600} \approx 0.4$, after which 10-fold serial dilutions were spotted onto regular

341 PYE agar or agarose (5-Azacytidine) plates containing the indicated concentrations of

342 Mitomycin C, Cisplatin, L-canavanine, Methyl methanosulfonate, and 4-Nitroquinoline N-oxide

343 (Sigma) followed by incubation at 30°C for 72 hours prior to imaging. Mitomycin C, L-

344 canavanine, and Cisplatin was prepared at a stock concentration of 0.4 mg/ml, 100 mg/ml, and

345 20 mM respectively in water followed by filter sterilization. 4-NQO was prepared at a saturated

346 solution in acetonitrile.

347

348 For synthetic lethality experiments with Lon depletion, xylose was present in all cultures at a

349 final concentration of 0.2%. Overnight cultures were back diluted to $OD_{600}$ 0.05 and outgrown

350 to $OD_{600} \approx 0.4$. Cells were 10-fold serially diluted, plated onto media containing 0.2% glucose

351 or 0.2 xylose, grown for 72 hours at 30°C and imaged.

352

353 Western Blot Analysis

354 Strains were cultured in PYE medium overnight. Cultures were diluted to $OD_{600}$ 0.05 and

355 grown to $OD_{600} \approx 0.4$. For steady state or translation shutoffs (30 μg/ml chloramphenicol) cells

356 were normalized and loaded onto a 10% BIS Tris pH 6.8 gel. Samples were run at 150V for 60
357 mins. Gels were transferred to nitrocellulose membranes at 100V for 50 minutes. Following
358 transfer, blots were blocked with TBST with 5% milk for 45 minutes and probed with anti-rabbit
359 primary CcrM, DnaA, and ClpP at 1:5,000 dilution overnight at 4°C. Blots were washed three
360 times for 5 minutes in TBST. Followed by incubation with Goat anti-rabbit LiCOR 800CW
361 secondary for 1 hour. Blots were washed three times in TBST and imaged using a LiCOR
362 Odyssey Imager, quantification was performed using ImageJ (NIH).
363
364 Worm strains and bacterial food sources
365 Hermaphrodite worms were raised on the OP50 strain of *E. coli* unless treated with *atfs-*
366 *1*(RNAi), in which the HT115 *E. coli* strain harboring the *atfs-1*(RNAi) plasmid was used
367 (Haynes et al., 2010). The $UPR^{mt}$ reporter worm strain harboring the *hsp-6*$_{pr}$*::gfp* transgene
368 used in the *C. elegans* imaging experiments was described previously (Yoneda et al., 2004).
369 All new strains were confirmed by sequencing, and backcrossed three times prior to crossing
370 into the *hsp-6*$_{pr}$*::gfp* background.
371
372 *C. elegans* cisplatin experiments
373 Worm strains were synchronized by bleaching. The eggs were transferred to plates containing
374 the described concentration of cisplatin (Sigma), allowed to hatch and develop for 36 hours,
375 when they were harvested and imaged as described (Nargund et al., 2012).
376
377 CRISPR/Cas9 genome editing
378 Via CRISPR-Cas9, a nucleic acid sequence encoding the amino acids -
379 GSDYKDDDDKGSDYKDDDDKGSDYKDDDDK-, which yields 3xFLAG epitope sites
380 (underlined) interspersed by -GS- linkers, was inserted at the 3' end of the endogenous *lonp-1*
381 open reading frame at the native locus as described (Friedland et al., 2013; Katic et al., 2015;

382 Paix et al., 2017). crRNAs and donor templates were generated and purchased from
383 Integrated DNA Technologies.
384
385 **LONP-1::FLAG**
386 crRNA sequence:
387 /AlTR1/rArArGrArArArGrGrGrArCrArCrGrUrArUrUrArUrGrUrUrUrUrArGrArGrCrUrArUrGrCrU/
388 AlTR2/
389 Donor template:
390 ATATTCGATTCGTTTCGCATTATGATGAGCTCTACGAGCATCTCTTCCAAGGATCCGACTA
391 CAAGGACGATGACGACAAGGGATCTGACTACAAGGACGATGACGACAAGGGATCTGACT
392 ACAAGGACGATGACGACAAGTAATAATACGTGTCCCTTTCTTTCACCCCCAGTTAATACCT
393 TTCAGATAGATTTTG
394
395 **LONP-1$^{4E}$**
396 To generate LONP-1$^{4E}$
397 Amino acid residues 467 (Arginine), 468 (Arginine), 473 (Lysine) and 474 (Lysine) were all
398 altered to aspartic acid residues via CRISPR-Cas9 as described above.
399 crRNA sequence:
400 /AlTR1/rArArCrUrGrArArArGrArCrGrArCrGrArUrUrCrUrGrUrUrUrUrArGrArGrCrUrArUrGrCrU/
401 AlTR2/
402
403 Donor template:
404 CTACCTGGAATGGTTGACATCAGTACCCTGGGGACTTACATCACCCGAGAATGAGGAACT
405 TTCAGTTGCAGAAGAGGCTCTTGATGAAGGACATTATGGA
406
407 <u>*C. elegans* western blots and mtDNA ChIP</u>

408 Western blots and ChIP experiments were performed as described (*51*), with several
409 modifications. Synchronized worms were cultured in liquid and harvested at the L4 stage by
410 sucrose flotation. Worms were resuspended in cold PBS + protease inhibitors (Roche) and
411 homogenized. The homogenate was treated with 1.85% formaldehyde for 15 min to cross-link
412 DNA and protein. Glycine was then added to a final concentration of 125mM for 5 min at room
413 temperature to quench the formaldehyde. The pellets were washed twice in cold PBS +
414 protease inhibitors, centrifuged at 2500 x G. Samples were sonicated using a Bioruptor
415 (Diagenode) for 15 min at 4°C on high intensity (30s on, 30s off). Samples were transferred to
416 microfuge tubes and spun at 13,000 x G for 15 min at 4°C. The supernatants were precleared
417 with pre-blocked ChIP-grade Pierce™ magnetic protein A/G beads (Thermo Scientific) and
418 then incubated with Monoclonal ANTI-FLAG® M2 antibody (Sigma, F1804) or Mouse mAb
419 IgG1 Isotype Control (Cell Signaling Technology, G3A1) overnight at 4°C. The antibody-
420 chromatin complex was then concentrated with pre-blocked ChIP-grade Pierce™ magnetic
421 protein A/G beads. After washing, DNA-protein crosslinks were reversed by incubation 65°C
422 overnight followed by treatment with RNaseA at 37°C for 2 hours, and then proteinase K at
423 55°C for 2 hours. Finally, immunoprecipitated and input DNA were purified with ChIP DNA
424 Clean & Concentrator (Zymo Research, D5205) and used as templates for qPCR. Relative
425 enrichment folds of detected regions were determined after normalization to input and total
426 mtDNA primers as described (Nargund et al., 2015).
427
428 qPCR primers to quantify *C. elegans* mtDNA following ChIP:
429 5'-GCAGTCTTAGCGTGAGGACATTA -3'
430 5'- AAACATAAAACATAAATAGAACTAACCA-3';
431
432 <u>Dynamic IPOD</u>

433 *In vivo* protein occupancy (IPOD) was measured as described (Freddolino et al., 2021) in
434 wildtype or Lon4E *Caulobacter crescentus* at initial and two hours after addition of
435 chloramphenicol to shut off translation. For Spearman correlation, occupancy scores were
436 averaged across overlapping 50 kb intervals across the genome and comparisons made
437 between timepoints and strains as shown. Wig files for occupancy data are provided in
438 Supplemental information.
439
440 **REFERENCES**

441


442 Bota, D.A., and Davies, K.J.A. (2002). Lon protease preferentially degrades oxidized
443 mitochondrial aconitase by an ATP-stimulated mechanism. Nature Cell Biology *4*, 674–680.

444 Charette, M.F., Henderson, G.W., Doane, L.L., and Markovitz, A. (1984). DNA-stimulated
445 ATPase activity on the lon (CapR) protein. J Bacteriol *158*, 195–201.

446 Chung, C.H., and Goldberg, A.L. (1982). DNA stimulates ATP-dependent proteolysis and
447 protein-dependent ATPase activity of protease La from Escherichia coli. Proc Natl Acad Sci U
448 S A *79*, 795–799.

449 Epshtein, V., Kamarthapu, V., McGary, K., Svetlov, V., Ueberheide, B., Proshkin, S., Mironov,
450 A., and Nudler, E. (2014). UvrD facilitates DNA repair by pulling RNA polymerase backwards.
451 Nature *505*, 372–377.

452 Freddolino, P.L., Amemiya, H.M., Goss, T.J., and Tavazoie, S. (2021). Dynamic landscape of
453 protein occupancy across the Escherichia coli chromosome. PLoS Biol *19*, e3001306.

454 Friedland, A.E., Tzur, Y.B., Esvelt, K.M., Colaiácovo, M.P., Church, G.M., and Calarco, J.A.
455 (2013). Heritable genome editing in C. elegans via a CRISPR-Cas9 system. Nat Methods *10*,
456 741–743.

457 Fu, G.K., Smith, M.J., and Markovitz, D.M. (1997). Bacterial Protease Lon Is a Site-specific
458 DNA-binding Protein. Journal of Biological Chemistry *272*, 534–538.

459 Goldberg, A.L. (1972). Degradation of abnormal proteins in Escherichia coli (protein
460 breakdown-protein structure-mistranslation-amino acid analogs-puromycin). Proc Natl Acad
461 Sci U S A *69*, 422–426.

462 Gora, K.G., Cantin, A., Wohlever, M., Joshi, K.K., Perchuk, B.S., Chien, P., and Laub, M.T.
463 (2013). Regulated proteolysis of a transcription factor complex is critical to cell cycle
464 progression in Caulobacter crescentus. Mol Microbiol *87*, 1277–1289.

465 Gray, M.W. (2012). Mitochondrial evolution. Cold Spring Harb Perspect Biol *4*, a011403–
466 a011403.

467 Gur, E., and Sauer, R.T. (2008). Recognition of misfolded proteins by Lon, a AAA(+) protease.
468 Genes Dev *22*, 2267–2277.

469 Haynes, C.M., Yang, Y., Blais, S.P., Neubert, T.A., and Ron, D. (2010). The matrix peptide
470 exporter HAF-1 signals a mitochondrial UPR by activating the transcription factor ZC376.7 in
471 C. elegans. Mol Cell *37*, 529–540.

472 Jenal, U., and Fuchs, T. (1998). An essential protease involved in bacterial cell-cycle control.
473 EMBO J *17*, 5658–5669.

474 Jonas, K., Liu, J., Chien, P., and Laub, M.T. (2013). Proteotoxic stress induces a cell-cycle
475 arrest by stimulating Lon to degrade the replication initiator DnaA. Cell *154*, 623–636.

476 Joshi, K.K., Bergé, M., Radhakrishnan, S.K., Viollier, P.H., and Chien, P. (2015). An Adaptor
477 Hierarchy Regulates Proteolysis during a Bacterial Cell Cycle. Cell *163*, 419–431.

478 Karlowicz, A., Wegrzyn, K., Gross, M., Kaczynska, D., Ropelewska, M., Siemiątkowska, M.,
479 Bujnicki, J.M., and Konieczny, I. (2017). Defining the crucial domain and amino acid residues
480 in bacterial Lon protease for DNA binding and processing of DNA-interacting substrates. J Biol
481 Chem *292*, 7507–7518.

482 Katic, I., Xu, L., and Ciosk, R. (2015). CRISPR/Cas9 Genome Editing in Caenorhabditis
483 elegans: Evaluation of Templates for Homology-Mediated Repair and Knock-Ins by Homology-
484 Independent DNA Repair. G3 (Bethesda) *5*, 1649–1656.

485 Liu, T., Lu, B., Lee, I., Ondrovičová, G., Kutejová, E., and Suzuki, C.K. (2004). DNA and RNA
486 Binding by the Mitochondrial Lon Protease Is Regulated by Nucleotide and Protein Substrate.
487 Journal of Biological Chemistry *279*, 13902–13910.

488 Lovett, S.T. (2011). The DNA Exonucleases of Escherichia coli. EcoSal Plus *4*.

489 Lu, B., Yadav, S., Shah, P.G., Liu, T., Tian, B., Pukszta, S., Villaluna, N., Kutejová, E.,
490 Newlon, C.S., Santos, J.H., et al. (2007). Roles for the Human ATP-dependent Lon Protease
491 in Mitochondrial DNA Maintenance. Journal of Biological Chemistry *282*, 17363–17374.

492 Margulis, L. (1970). Origin of eukaryotic cells: evidence and research implications for a theory
493 of the origin and evolution of microbial, plant, and animal cells on the Precambrian earth (New
494 Haven: Yale University Press).

495 Mizusawa, S., and Gottesman, S. (1983). Protein degradation in Escherichia coli: the lon gene
496 controls the stability of sulA protein. Proc Natl Acad Sci U S A *80*, 358–362.

497 Nargund, A.M., Pellegrino, M.W., Fiorese, C.J., Baker, B.M., and Haynes, C.M. (2012).
498 Mitochondrial import efficiency of ATFS-1 regulates mitochondrial UPR activation. Science
499 *337*, 587–590.

500 Nargund, A.M., Fiorese, C.J., Pellegrino, M.W., Deng, P., and Haynes, C.M. (2015).
501 Mitochondrial and nuclear accumulation of the transcription factor ATFS-1 promotes OXPHOS
502 recovery during the UPR(mt). Mol Cell *58*, 123–133.

503 Ogawa, H., Shimada, K., and Tomizawa, J. (1968). Studies on radiation-sensitive mutants of
504 E. coli: I. Mutants defective in the repair synthesis. Molec. Gen. Genet. *101*, 227–244.

505 Paix, A., Folkmann, A., and Seydoux, G. (2017). Precision genome editing using CRISPR-
506 Cas9 and linear repair templates in C. elegans. Methods *121–122*, 86–93.

507 Petrova, V., Chen, S.H., Molzberger, E.T., Tomko, E., Chitteni-Pattu, S., Jia, H., Ordabayev,
508 Y., Lohman, T.M., and Cox, M.M. (2015). Active displacement of RecA filaments by UvrD
509 translocase activity. Nucleic Acids Res *43*, 4133–4149.

510 Reinking, H.K., Hofmann, K., and Stingele, J. (2020). Function and evolution of the DNA-
511 protein crosslink proteases Wss1 and SPRTN. DNA Repair (Amst.) *88*, 102822.

512 Veaute, X., Delmas, S., Selva, M., Jeusset, J., Le Cam, E., Matic, I., Fabre, F., and Petit, M.-A.
513 (2005). UvrD helicase, unlike Rep helicase, dismantles RecA nucleoprotein filaments in
514 Escherichia coli. EMBO J *24*, 180–189.

515 Vieux, E.F., Wohlever, M.L., Chen, J.Z., Sauer, R.T., and Baker, T.A. (2013). Distinct
516 quaternary structures of the AAA+ Lon protease control substrate degradation. Proc Natl Acad
517 Sci U S A *110*, E2002–E2008.

518 Witkin, E.M. (1946). Inherited Differences in Sensitivity to Radiation in Escherichia Coli. Proc
519 Natl Acad Sci U S A *32*, 59–68.

520 Wright, R., Stephens, C., Zweiger, G., Shapiro, L., and Alley, M.R. (1996). Caulobacter Lon
521 protease has a critical role in cell-cycle control of DNA methylation. Genes & Development *10*,
522 1532–1542.

523 Yoneda, T., Benedetti, C., Urano, F., Clark, S.G., Harding, H.P., and Ron, D. (2004).
524 Compartment-specific perturbation of protein handling activates genes encoding mitochondrial
525 chaperones. J. Cell Sci. *117*, 4055.

526 Zehnbauer, B.A., Foley, E.C., Henderson, G.W., and Markovitz, A. (1981). Identification and
527 purification of the Lon+ (capR+) gene product, a DNA-binding protein. Proc Natl Acad Sci U S
528 A *78*, 2043–2047.

529 Zeinert, R.D., Baniasadi, H., Tu, B.P., and Chien, P. (2020). The Lon Protease Links
530 Nucleotide Metabolism with Proteotoxic Stress. Mol. Cell.

531

532 SUPPLEMENTAL INFORMATION

533 **Supplemental Figure Legends.**

534

535 **Figure S1**. Supporting main Figure 1. **A.** Three biological replicates of wildtype, ∆lon and
536 Lon4E strains were individually grown to exponential phase. Cell length and stalk were
537 measured for each. Cell lengths were determined automatically using MicrobeJ, Stalk lengths
538 were measured manually using ImageJ (NIH). Individual measurements are shown as well as
539 a notched box plot for these values. **B.** Growth in 0.3% Agar PYE media of WT, ∆lon and
540 Lon4E strains on left. Western blot of labeled proteins shown on right. **C.** Degradation of
541 CcrM is restored in Lon4E. Chloramphenicol was added to exponentially growing cells and
542 timepoints were taken at timepoints indicated. Quantification was performed as described in
543 methods (n=3). **D.** Purified Lon or Lon4E can degrade fluorescently labeled casein (FITC-
544 casein; Sigma) with similar efficiency. Degradation of FITC-casein results in increased
545 fluorescence due to loss of self-quenching. Lon binding to certain single-stranded DNA
546 oligonucleotides suppresses degradation of FITC-casein, but Lon4E is not responsive. **E.**
547 Additional concentrations and replicates of growth under stress similar to main Figure 1.

548

# Figure S1

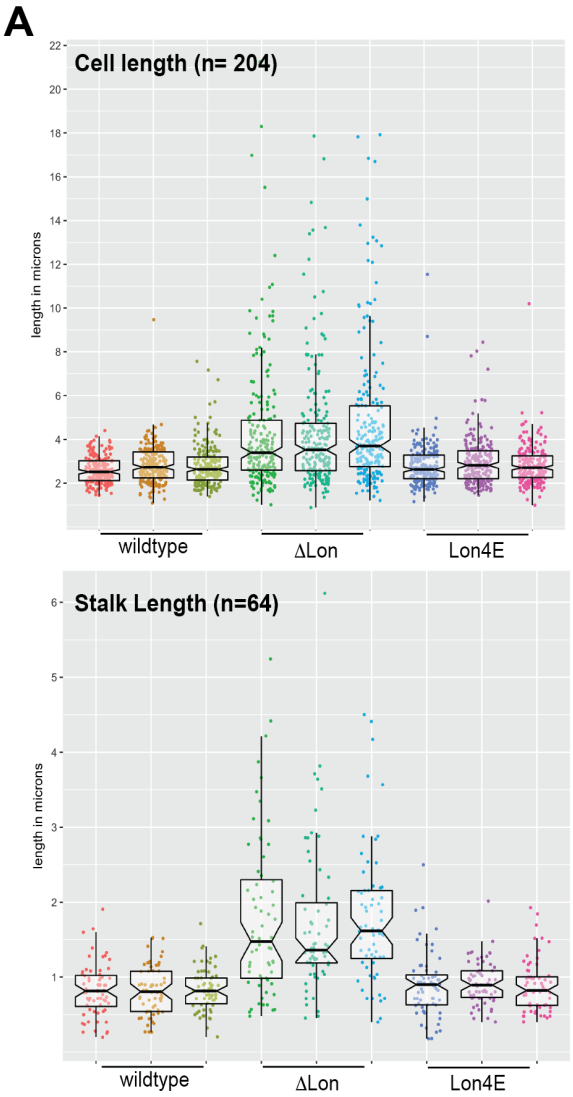
A
Cell length (n= 204)
length in microns
wildtype
ΔLon
Lon4E
Stalk Length (n=64)
length in microns
wildtype
ΔLon
Lon4E

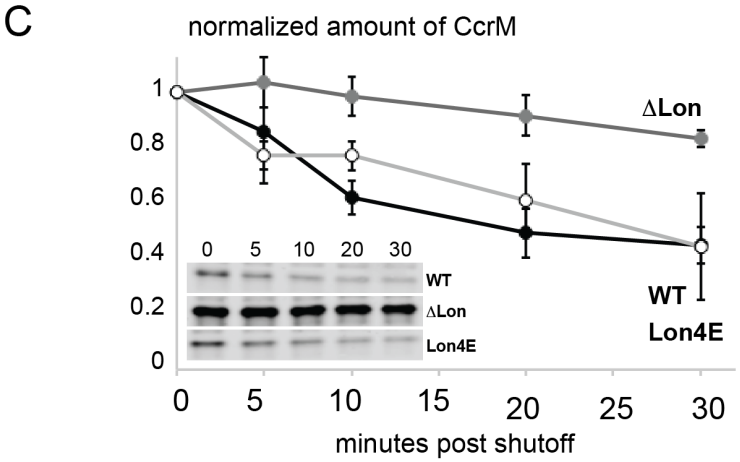
C
normalized amount of CcrM
ΔLon
WT
Lon4E
0 5 10 20 30
WT
ΔLon
Lon4E
minutes post shutoff

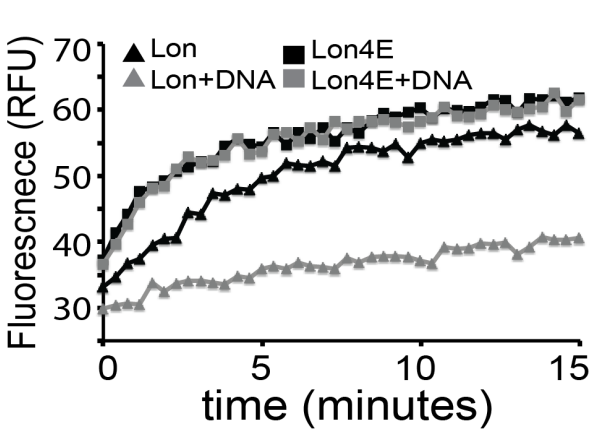
D
Lon
Lon+DNA
Lon4E
Lon4E+DNA
Fluorescnece (RFU)
time (minutes)

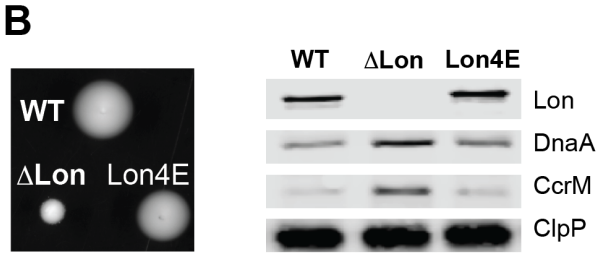
B
WT
ΔLon
Lon4E
WT
ΔLon
Lon4E
Lon
DnaA
CcrM
ClpP

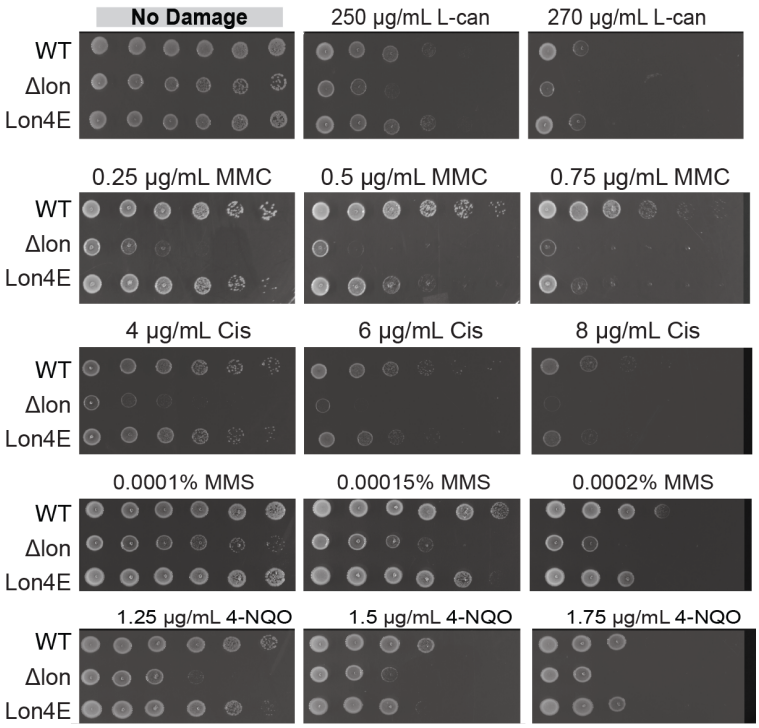
E
No Damage
250 µg/mL L-can
270 µg/mL L-can
0.25 µg/mL MMC
0.5 µg/mL MMC
0.75 µg/mL MMC
4 µg/mL Cis
6 µg/mL Cis
8 µg/mL Cis
0.0001% MMS
0.00015% MMS
0.0002% MMS
1.25 µg/mL 4-NQO
1.5 µg/mL 4-NQO
1.75 µg/mL 4-NQO
WT
Δlon
Lon4E

549

550 **Figure S2.** Supporting main Figure 2. Cells expressing a xylose inducible Lon as the sole copy

551 (Δ*lon Pxyl:lon*) can tolerate loss of *uvrD* under inducing, but not repressing conditions.

552 Similarly, depletion of Lon in a Δ*exoVII* strain also results in reduced fitness. Loss of Lon

553 shows no synthetic effects with loss of *recA*, *imuB* or *mmcA*, although loss of these genes

554 dramatically increases sensitivity to DNA damage produced by mitomycin C.

555

**Figure S2**

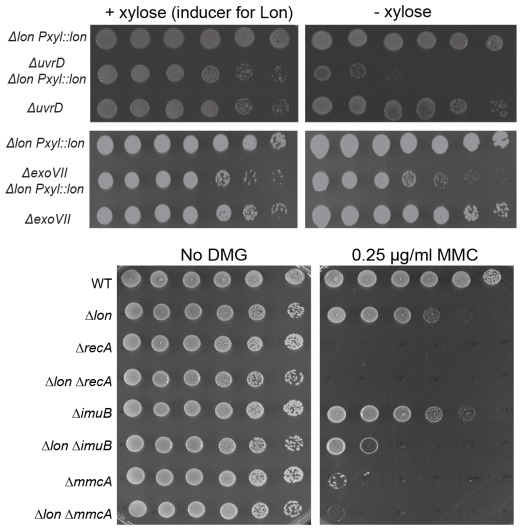
+ xylose (inducer for Lon)
- xylose
ΔIon Pxyl::Ion
ΔuvrD
ΔIon Pxyl::Ion
ΔuvrD
ΔIon Pxyl::Ion
ΔexoVII
ΔIon Pxyl::Ion
ΔexoVII
No DMG
0.25 µg/ml MMC
WT
ΔIon
ΔrecA
ΔIon ΔrecA
ΔimuB
ΔIon ΔimuB
ΔmmcA
ΔIon ΔmmcA

556

557 **Figure S3.** Supporting main Figure 3. A. CtrA degradation in WT, Lon4E and ∆lon strains with

558 and without mitomycin C damage. B. Degradation of DnaA by dsDNA is increased with WT

559 Lon, but not with Lon4E. n.b., DnaAR357A is used here as it is unable to hydrolyze ATP and

560 therefore is persistently locked in the ATP-bound / DNA-binding state.

561

# Figure S3

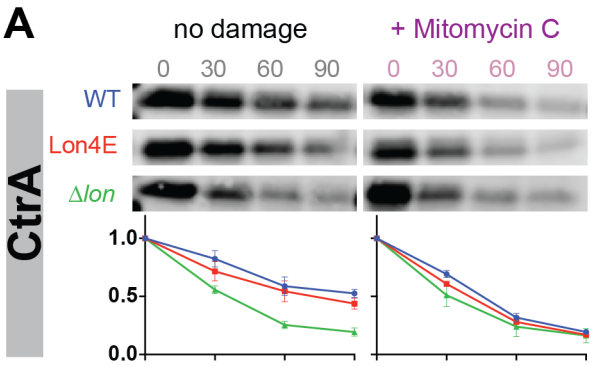
A
no damage
+ Mitomycin C
0 30 60 90
0 30 60 90
WT
Lon4E
Δlon
CtrA
1.0
0.5
0.0

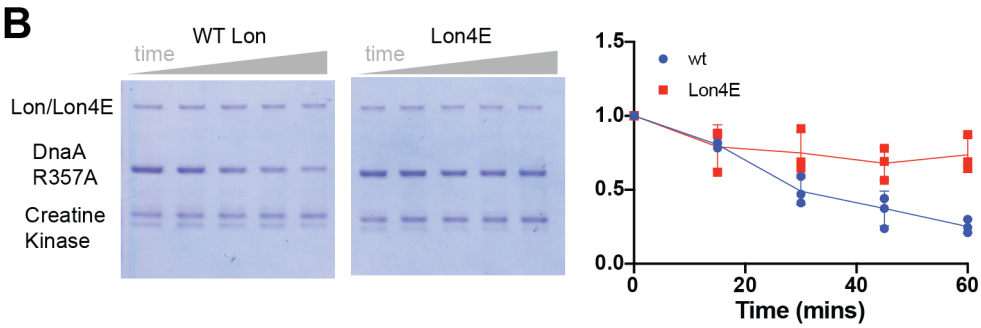
B
WT Lon
Lon4E
time
time
Lon/Lon4E
DnaA
R357A
Creatine
Kinase
1.5
1.0
0.5
0.0
wt
Lon4E
0
20
40
60
Time (mins)